Progress In Electromagnetics Research M, Vol. 106, 47–57, 2021

Single-Feed Cylindrical Dielectric Resonator Antenna with Wide Angular Circular Polarization

Hongmei Liu*, Tuanyuan Yan, Shaojun Fang, and Zhongbao Wang

Abstract—In this paper, a single-feed cylindrical dielectric resonator antenna (DRA) with wide angular circular polarization is proposed. It is composed of a cylindrical cavity loaded cylindrical dielectric resonator (DR), an orthogonal slot with curved arms, and an off-centered L-shaped microstrip line. By inserting the slot with curved arms and a cylindrical cavity, the 3-dB axial ratio beamwidth (ARBW) can be increased, and symmetric radiation can be obtained. For validation, a prototype is designed and fabricated. The overall size is $0.39\lambda_0 \times 0.39\lambda_0 \times 0.13\lambda_0$. The measured results show that it exhibits a 10-dB impedance bandwidth of 33.3% (1.45 $\sim$ 2.03 GHz) with a circularly polarized (CP) bandwidth of 16.1% (1.54 $\sim$ 1.81 GHz). Symmetric radiations are obtained, and the 3-dB ARBWs in the *xoz* and *yoz* planes are more than 150° over the CP bandwidth.

1. INTRODUCTION

Dielectric resonator antennas (DRAs) are widely applied in wireless communication systems due to the advantages of high radiation efficiency, low cost, and light weight [1–3]. Reconfigurability can also be realized using liquid-based DRAs [4, 5]. In recent years, the requirements of circularly polarized (CP) DRAs have been boosted over the linearly polarized (LP) ones since CP antennas are more immune to multipath distortion and polarization mismatch. In general, the method for implementing a CP DRA can be classified as single-feed and dual-feeds. For the dual-feed method, the dimensions and complexity will be increased by the external feed networks such as quadrature coupler and power divider. On the other hand, the feed network for single-feed is usually simpler. In [6], a single aperture coupled feed DRA is proposed, and the circular polarization is obtained by rotated stacked DRAs. In [7], the geometry of a cylindrical DRA is deformed periodically along the azimuthal direction to generate circular polarization. In [8], a filtering elliptical DRA with two notches is proposed and excited by a V-shaped copper strip to facilitate CP operation. Simpler methods such as off-centered microstrip line [9], semi-eccentric annular DR [10], and helical exciter [11] are also reported. However, they all exhibit narrow 3-dB axial ratio (AR) bandwidth (less than 8%).

To increase the CP bandwidth, different techniques are applied including modifying the structures of the dielectric resonators (DRs) and the feedings. In [12] and [13], a Spidron fractal DR and a rotated-stair DR are used, and the 3-dB AR bandwidths are increased to 11.57% and 18.02%, respectively. In [14] and [15], a question-mark-shaped microstrip line and an Archimedean spiral slot are applied to obtain a 3-dB AR bandwidth of about 25%. In [16], a cylindrical DRA excited by a modified circular-shaped aperture is presented, and the CP bandwidths are enhanced at four frequency bands. Moreover, DRAs with further enhanced CP bandwidth can also be realized by applying complex structures, such as rectangular and half split cylindrical DRs with stair-shaped slot feeding [17], stair-shaped DR with open-ended slot ground [18], square DR with two unequal inclined slits [19], a cylindrical DR with substrate-integrated embedded [20], a rectangular DRA excited by a conformal H-shaped metal strip [21], two

Received 20 September 2021, Accepted 24 November 2021, Scheduled 1 December 2021
* Corresponding author: Hongmei Liu (lhm323@dlmu.edu.cn).
The authors are with the School of Information Science and Technology, Dalian Maritime University, Dalian 116026, Liaoning, China.

connected DRs excited by an offset vertical metallic strip [22], a stacked DRA with high and low permittivities [23], and a square DR with four vertical metallic plates [24]. Except the CP bandwidth, wide angular circular polarization and stable radiation patterns with no multi-lobes in the main beam are two other critical features of CP antennas, which have been a challenging task and an emerging research topic. However, to the authors' knowledge, less efforts have been found.

In the paper, a single-feed cylindrical DRA with wide angular circular polarization is proposed. Wide angular circular polarization with symmetric radiation is realized by inserting an orthogonal slot with curved arms and a cylindrical cavity. The measured results show that the proposed DRA exhibits 3-dB ARBWs of more than 150° in the xoz and yoz planes over the 3-dB AR bandwidth of 16.1%.

2. ANTENNA CONFIGURATION AND DESIGN

2.1. Antenna Design

Figure 1 shows the geometry of the proposed CP DRA, which consists of a cylindrical cavity loaded cylindrical DR, an orthogonal slot with curved arms, and an off-centered L-shaped microstrip line. The cylindrical DR ($\varepsilon_r = 10$) with radius of R_2 and height of h_2 is placed on the center of an FR_4 epoxy ($\varepsilon_r = 4.4$) substrate with the dimensions of $W_0 \times L_0$ and thickness of 1.5 mm. Dimensions of the DR are selected to operate at the fundamental mode. In the middle of the cylindrical DR, a cylindrical cavity with radius of R_1 and height of h_3 is inserted. Excitation is applied using a 50 Ω L-shaped microstrip line with dimensions $W_1 \times (L_1 + L_2)$. The distance between the microstrip line and the substrate center is d_1. To achieve CP radiations, an orthogonal slot with dimensions of $W_2 \times L_5$ is etched on the ground plane. Besides, arc-shaped slots with radians of α_1, α_2, α_3, and α_4 are loaded on the orthogonal slot for improving the AR performance.

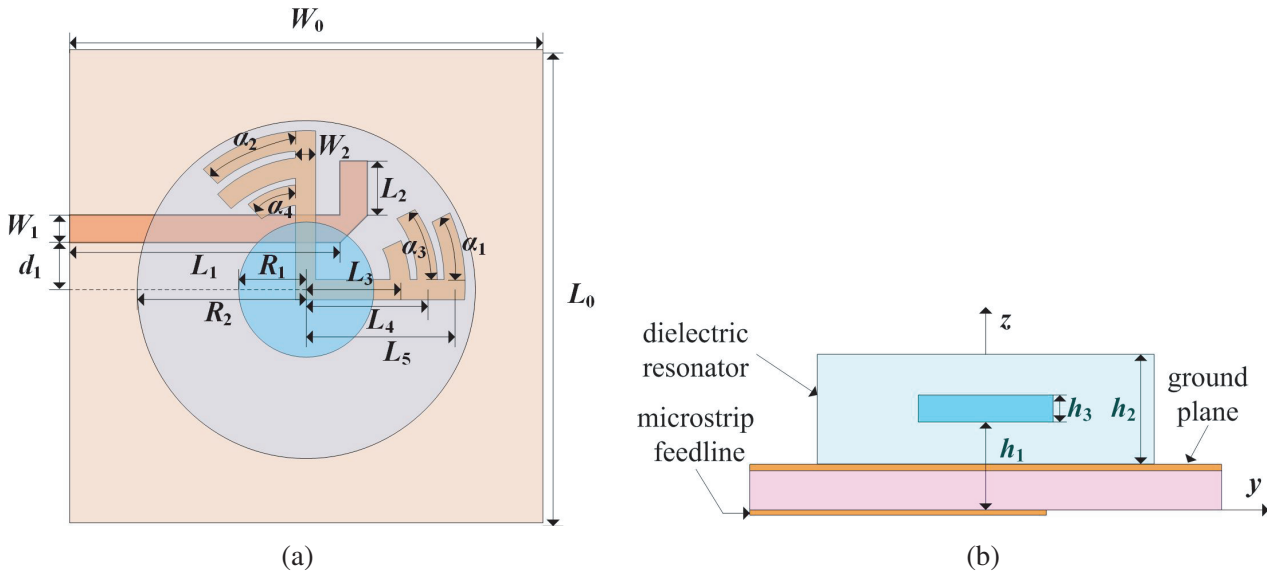

Figure 1. Structure of proposed DRA. (a) Top view. (b) Side view.

2.2. Operating Principle

In this section, a DRA operating at L-band is designed for validation. Table 1 shows the optimized dimensions of the designed DRA. Fig. 2 shows the E-field distributions of the designed DRA, and the frequency of 1.7 GHz is chosen for exhibition. It is observed that the E-field is in the anticlockwise direction as the angular time increases, which indicates that the radiation in the $+z$-direction is right-hand CP (RHCP). In this section, by comparing with two reference antennas, the principle of the proposed DRA is explained. As shown in Fig. 3(a), Ant. 1 is a cylindrical DRA fed by orthogonal slots

Table 1. Dimensions of the proposed DRA (UNIT: mm).

Parameter	Value	Parameter	Value	Parameter	Value
L	70	W_2	3	R_2	25
W	70	L_3	14	d_1	7
L_1	40	L_4	18	h_1	10
W_1	4	L_5	22	α_1	36°
L_2	8	R_1	10	α_2	30°
h_3	3	h_2	23	α_3	40°
α_4	30°				

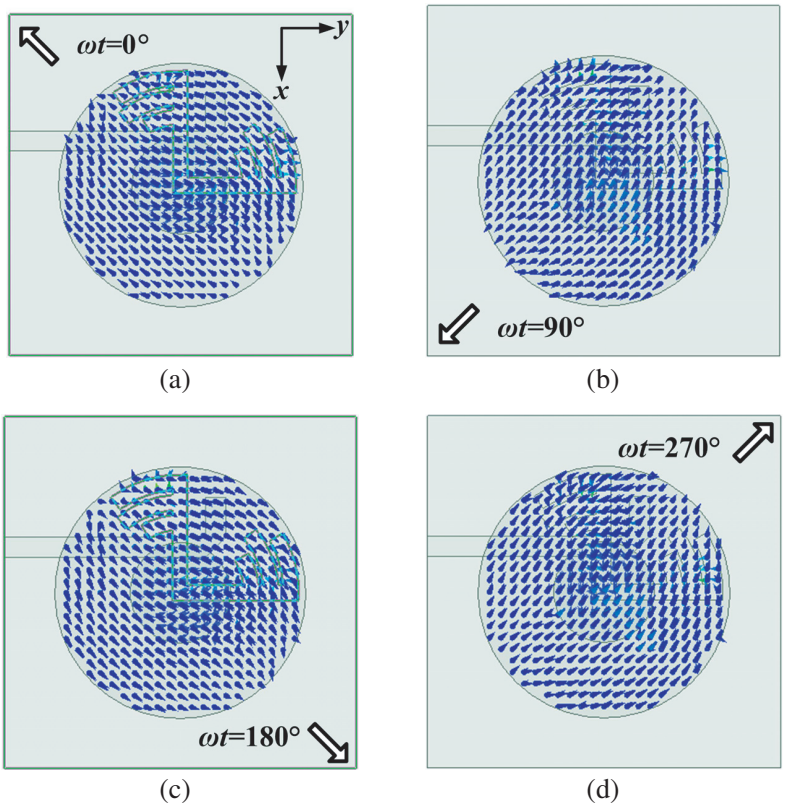

Figure 2. E-field distribution in the cylindrical DR. (a) $\omega t = 0°$. (b) $\omega t = 90°$. (c) $\omega t = 180°$. (d) $\omega t = 270°$.

with dimensions of $W_2 \times L_5$. Since the CP wave is excited by two orthogonal LP components with equal amplitude and 90° phase difference, an initial estimation of the dimensions of the aperture slot L_5 and the feed location d_1 are obtained from the following equations [25]:

$$L_5 - d1 = \frac{\lambda_0}{2\sqrt{\varepsilon_{\text{eff}}}} \tag{1}$$

$$L_5 + d1 = \frac{3\lambda_0}{4\sqrt{\varepsilon_{\text{eff}}}} \tag{2}$$

where λ_0 is the wavelength at the center frequency, and ε_{eff} is the effective permittivity. The optimized parameters of the antenna are obtained by simulator Ansoft HFSS. Fig. 4 shows the comparisons of

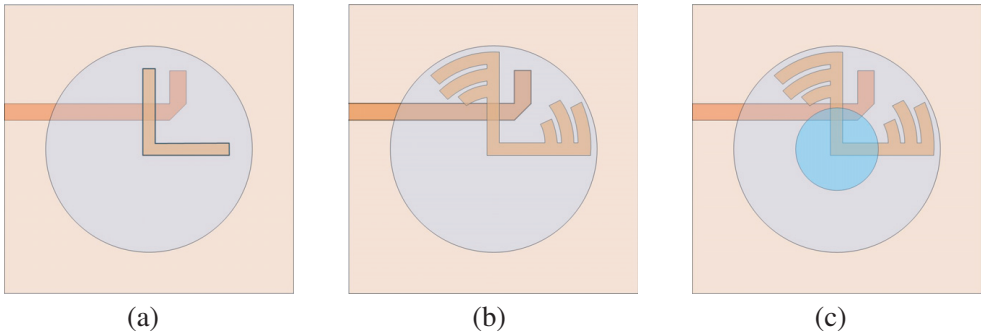

Figure 3. Antenna design evolution. (a) Ant. 1. (b) Ant. 2. (c) Ant. 3.

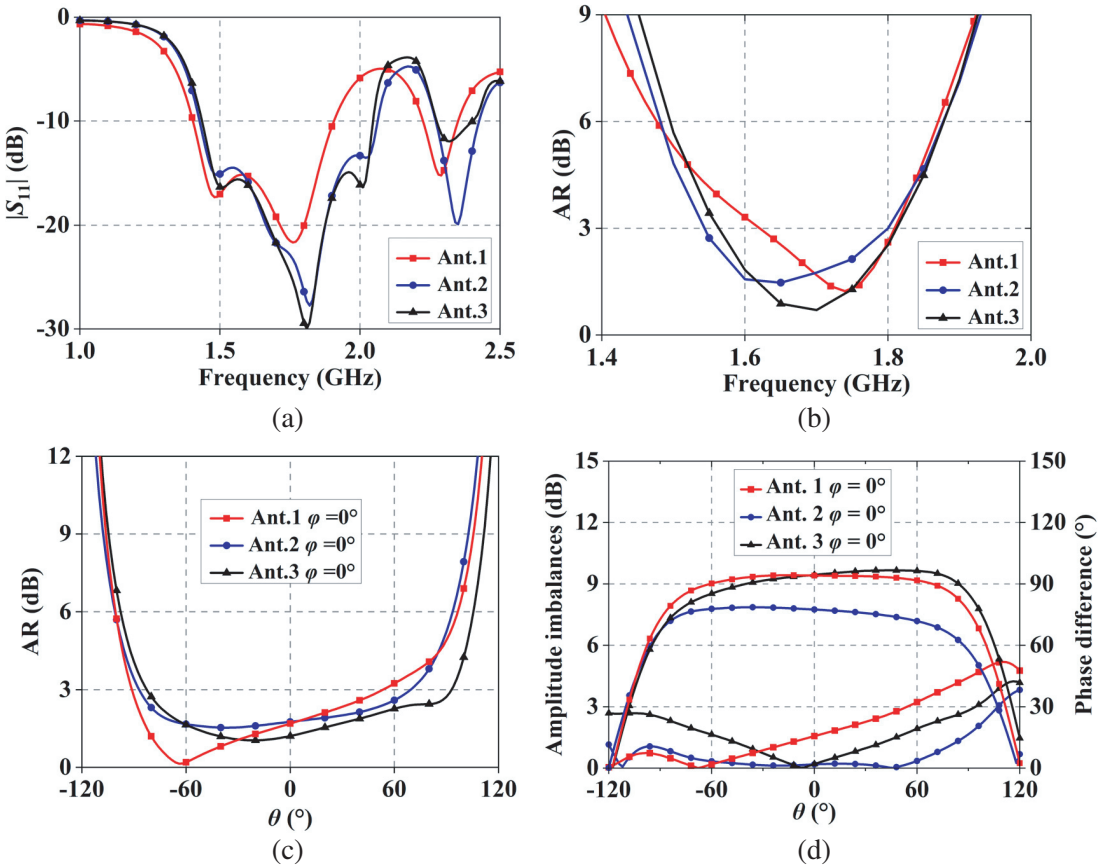

Figure 4. Comparisons of different antenna evolutions. (a) $|S_{11}|$. (b) AR. (c) ARBWs. (d) Amplitude imbalances and phase differences of E_θ and E_ϕ.

$|S_{11}|$ and AR performances. It is observed that the fractional bandwidths (FBWs) for Ant. 1 under the criterions of $|S_{11}| < 10$ dB and AR < 3 dB are 30.8% (1.401.91 GHz) and 11.1% (1.621.81 GHz), respectively. The 3-dB ARBW at xoz plane ($\phi = 0°$) is 144.7°. The reason for narrow and asymmetric ARBW is the poor performance of amplitude imbalance, as shown in Fig. 4(d).

To improve the impedance bandwidth and AR performance, three extra arc-shaped slots are etched on each of the orthogonal slots (named as Ant. 2), as shown in Fig. 3(b). Here, the radians of the outermost two slots are α_1 and α_2, respectively. The middle slots have the same radian of α_3, and the innermost slots have the same radian of α_4. By inserting the extra slots, the alignment of the excitation

field is enhanced which will increase the AR bandwidth. Besides, the ARBW is also improved since the arc-shaped slots contribute to the CP radiation at low elevation angles. It is seen from Fig. 4(b) that the 3-dB AR bandwidth is increased to 16% (1.541.80 GHz) with an improved impedance bandwidth of 36% (1.432.06 GHz). As can be seen from Fig. 4(d), since the performance of amplitude imbalance is improved, a symmetric ARBW is obtained. However, due to the decrease of the phase difference, the 3-dB ARBW is only enhanced to 156°.

To adjust the phase difference of the antenna, a cylindrical cavity with radius of R_1 and height of h_3 is inserted (named as Ant. 3), as shown in Fig. 3(c). According to the CP wave refraction theory between two different dielectrics [26], the CP wave is refracted three times before radiating into the space due to the introduction of the cylindrical cavity. The polar angle of CP wave is changed because of the refraction which in return modifies the phase difference of the antenna. Therefore, by adjusting the dimension of the cylindrical cavity, the AR at certain polar angle in free space can be improved to wide angle range. It is seen from Fig. 4(d) that the phase difference is obviously increased to about 90° by using the cylindrical cavity. Although the amplitude imbalance is deteriorated compared with Ant. 2, the CP radiation relies more on the phase difference than the amplitude. It can be verified from Fig. 4(c) that the 3-dB ARBW for Ant. 3 is increased to 171°.

3. NUMERICAL ANALYSIS FOR THE ANTENNA

The influences of antenna parameters on the performance of $|S_{11}|$ and AR performance are analyzed and optimized. In the process of parameter analysis, other parameters are maintained at their optimized values. The plotted ARBWs are all at the xoz plane of 1.7 GHz.

3.1. Effects of the Arc-Shaped Slots

Since the arc-shaped slots mainly affect the AR performance of the antenna, the simulated results for 3-dB AR bandwidth and 3-dB ARBW are plotted for comparison. Fig. 5 shows the influences of the radians for the outermost two slots (α_1 and α_2). It is found that the AR bandwidth and 3-dB ARBW are both increased with the increase of α_2 from 20° to 40°. When the value of α_2 is in the range of 20° $\sim$ 25°, the widest AR bandwidth and 3-dB ARBW can be obtained at $\alpha_1 = 40°$. Fig. 6 shows the influences of the radian for the middle slots (α_3). It is observed that narrow 3-dB AR bandwidth and 3-dB ARBW are obtained when α_3 is larger than 40°. When α_3 increases from 30° to 40°, both the 3-dB AR bandwidth and 3-dB ARBW are slightly narrowed. Fig. 7 shows the influences of the radian for the innermost slots (α_4). It is observed that when α_4 increases from 20° to 35°, the 3-dB AR bandwidth is decreased. While the 3-dB ARBWs are nearly unchanged with α_4, only the AR value at $\theta = 0°$ is decreased.

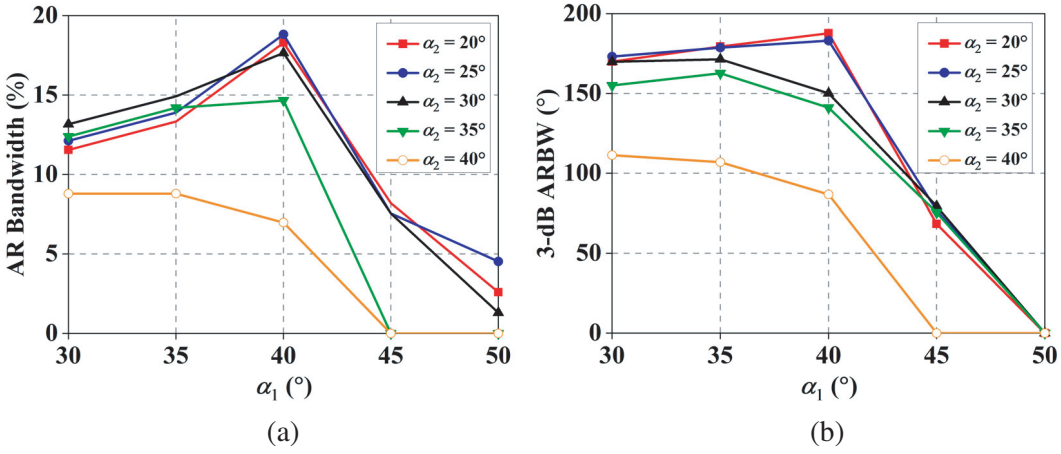

Figure 5. Effects of α_1 and α_2 on (a) AR bandwidth and (b) 3-dB ARBW.

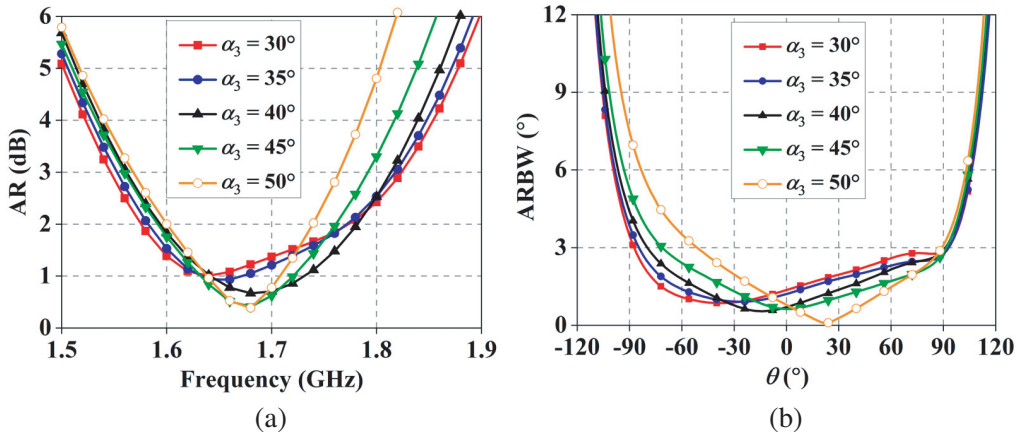

Figure 6. Effects of α_3 on (a) AR and (b) ARBW.

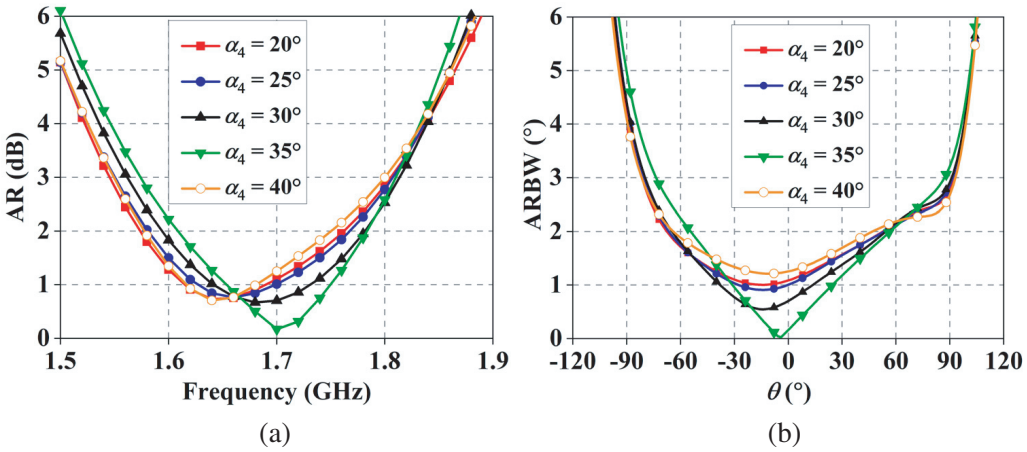

Figure 7. Effects of α_4 on (a) AR and (b) ARBW.

3.2. Effects of the Cylindrical Cavity

In this section, the radius (R_1) and height (h_3) of the cylindrical cavity are investigated. Fig. 8 shows the effects of the radius (R_1) on the AR and ARBW performances of the antenna. It is seen that both

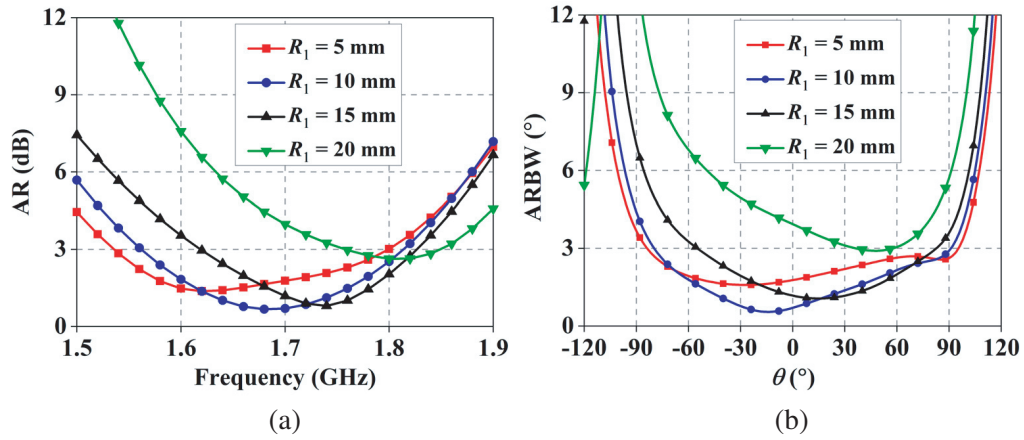

Figure 8. Effects of R_1 on (a) AR and (b) ARBW.

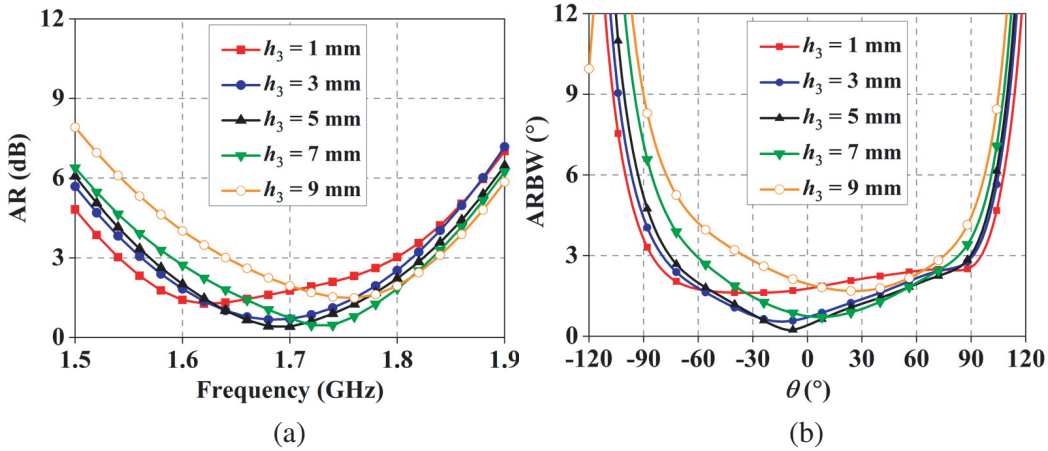

Figure 9. Effects of h_3 on (a) AR and (b) ARBW.

the CP bandwidth and 3-dB ARBW are narrowed along with the increase of R_1. The widest and better CP bandwidth and 3-dB ARBW are obtained at $R_1 = 10$ mm. Fig. 9 shows the effects of the height (h_3). The CP bandwidth and 3-dB ARBW are narrowed when h_3 is larger than 5 mm. In the range of $1 \sim 5$ mm, better performance can be obtained at $h_3 = 3$ mm or 5 mm.

4. EXPERIMENTAL VERIFICATION

To validate the proposed CP DRA, a prototype has been fabricated, as shown in Fig. 10. The Agilent N5230A vector network analyzer and an anechoic chamber have been used to measure the fabricated prototype. The simulated and measured $|S_{11}|$, AR, and gain performances are plotted in Fig. 11. It is seen that the simulated and measured FBWs for $|S_{11}| < 10$ dB are 35.2% (1.45 $\sim$ 2.07 GHz) and 33.3% (1.45 $\sim$ 2.03 GHz), respectively. The values for AR < 3 dB are 15.5% (1.55 $\sim$ 1.81 GHz) and 16.1% (1.54 $\sim$ 1.81 GHz), respectively. In the entire AR bandwidth, the measured gain is more than 4.6 dBic with a peak gain of 5.1 dBic at 1.7 GHz. Fig. 12 shows the simulated and measured radiation patterns in the *xoz* and *yoz* planes. Good agreements are observed between the simulated and measured results with symmetric radiations. Fig. 13 shows the simulated and measured ARBWs at 1.7 GHz and 1.65 GHz. At the *xoz* plane, the measured ARBWs are 162° at 1.65 GHz and 172° at 1.7 GHz, while the values are 152° and 182° at the *yoz* plane.

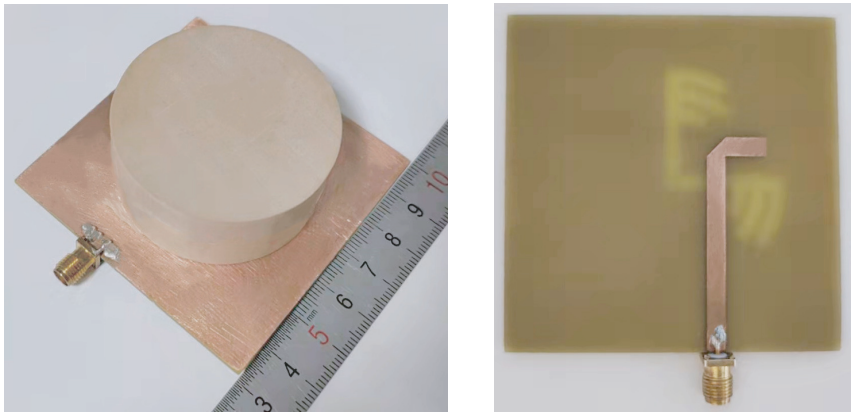

Figure 10. Photograph of the prototype. (a) Top view. (b) Bottom view.

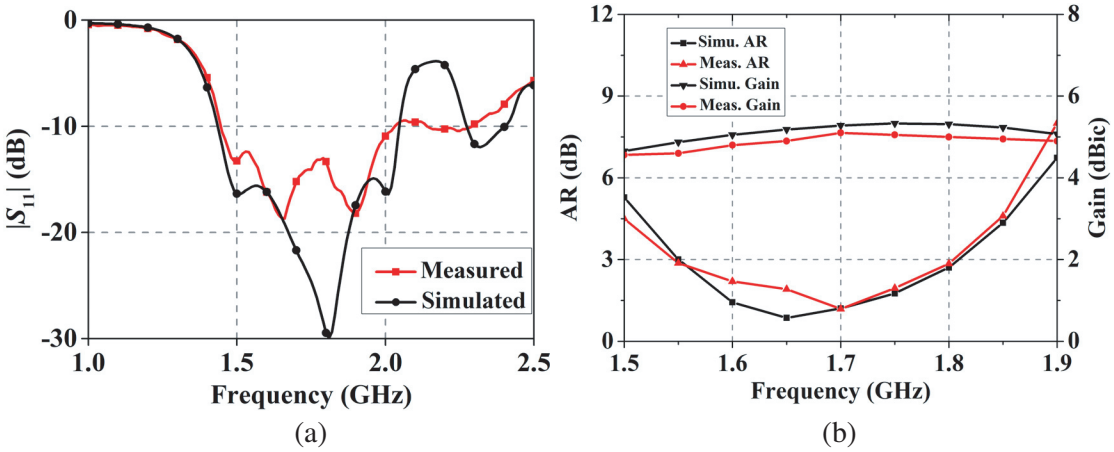

Figure 11. Measured and simulated results. (a) $|S_{11}|$. (b) AR and Gain.

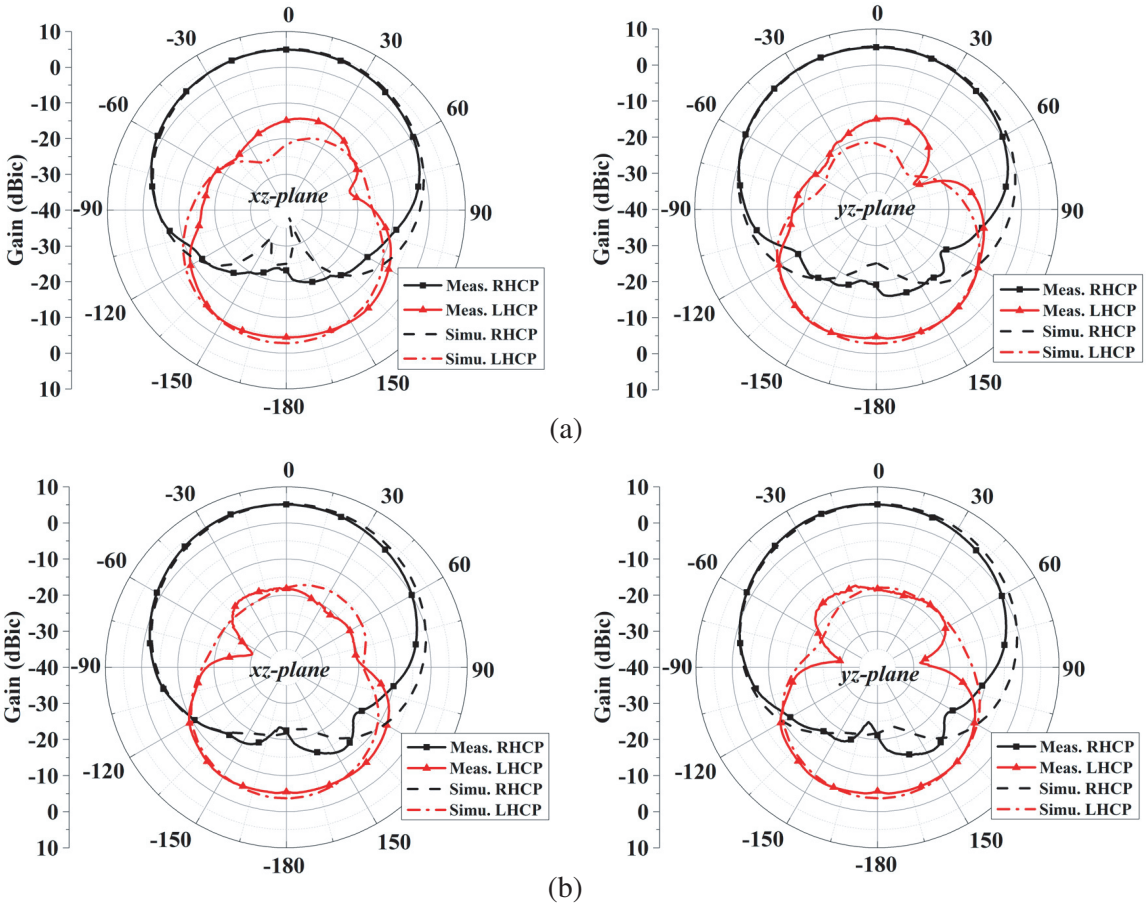

Figure 12. Simulated and measured radiation patterns at (a) 1.65 GHz and (b) 1.7 GHz.

Table 2 shows the comparisons of the proposed DRA with several representative antennas. It is observed that compared with the listed DRAs, the proposed DRA shows wider ARBW of larger than 150° in both *xoz* and *yoz* planes, which can be used for receiving CP signals stably. Smaller dimension is also the advantage of the proposed DRA.

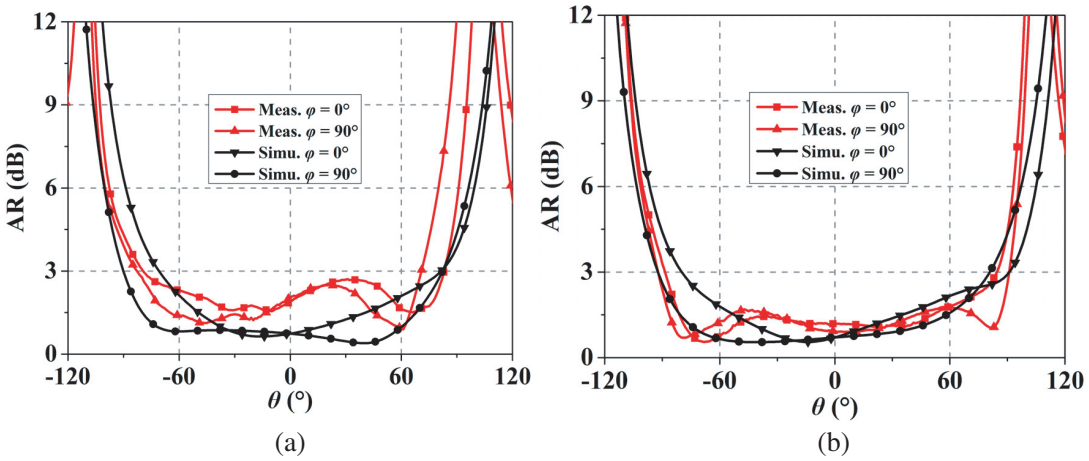

Figure 13. Simulated and measured ARBWs at (a) 1.65 GHz and (b) 1.7 GHz.

Table 2. Comparison with representative DRAs.

Ref.	FBW (%)	CP Bandwidth (%)	3-dB ARBW (°)	Size ($\lambda_0 \times \lambda_0 \times \lambda_0$)
[4]	12.82	7.64	< 40	$0.62 \times 0.62 \times 0.15$
[5]	23.8	23.8	< 60	$1.31 \times 1.31 \times 0.32$
[7]	51.2	8.01	< 60	$0.72 \times 0.72 \times 0.25$
[8]	4.1	4.1	< 60	$0.81 \times 0.81 \times 0.14$
[10]	29.1	5.7	< 50	$1.25 \times 1.25 \times 0.16$
[17]	49.67	41.01	114	$1.47 \times 1.47 \times 0.09$
[20]	33.5	26.3	< 60	$1.03 \times 1.03 \times 0.12$
[21]	27.7	20	< 90	$0.34 \times 0.19 \times 0.35$
[22]	69.66	44.73	< 90	$0.43 \times 0.49 \times 0.41$
[23]	25.4	22.8	< 90	$1.01 \times 1.01 \times 0.16$
Proposed	**33.3**	**16.1**	**> 150**	**$0.39 \times 0.39 \times 0.13$**

λ_0 is the wavelength in air at the center frequency.

5. CONCLUSION

In this paper, a single-feed cylindrical DRA with wide angular circular polarization is proposed. Wide angular circular polarization with symmetric radiation is realized by inserting a slot with curved arms and a cylindrical cavity. The measured results show that the proposed DRA has a 10-dB impedance bandwidth of 33.3% with a CP bandwidth of 16.1%. Over the CP bandwidth, the 3-dB ARBWs in the *xoz* and *yoz* planes are more than 150°, which is much larger than the 3-dB ARBW of the reported DRAs. Due to the good CP performance, the antenna can be redesigned at arbitrary frequency and applied in applications that need wide angular circular polarization.

ACKNOWLEDGMENT

This work was supported in part by the National Natural Science Foundation of China under Grant 51809030 and Grant 61871417, in part by the Natural Science Foundation of Liaoning Province under Grant 2020-MS-127, in part by the Liaoning Revitalization Talents Program under Grant XLYC2007067, in part by the Dalian Youth Science and Technology Star Project under Grant 2020RQ007 and in part by the Fundamental Research Funds for the Central Universities under Grant 3132021231.

REFERENCES

1. Zhao, Z., J. Ren, Y. Liu, Z. Zhou, and Y. Yin, "Wideband dual-feed, dual-sense circularly polarized dielectric resonator antenna," *IEEE Trans. Antennas Propag.*, Vol. 68, No. 12, 7785–7793, Dec. 2020.
2. Vahora, A. and K. Pandya, "Implementation of cylindrical dielectric resonator antenna array for Wi-Fi/wireless LAN/satellite applications," *Progress In Electromagnetics Research M*, Vol. 90, 157–166, 2020.
3. Pimpalgaonkar, P. R., et al., "A review on dielectric resonator antenna," *1st International Conference on Automation in Industries (ICAI)*, 106–109, 2016.
4. Wang, M. and Q. Chu, "A wideband polarization-reconfigurable water dielectric resonator antenna," *IEEE Antennas Wireless Propag. Lett.*, Vol. 18, No. 2, 402–406, Feb. 2019.
5. Ren, J., et al., "Radiation pattern and polarization reconfigurable antenna using dielectric liquid," *IEEE Trans. Antennas Propag.*, Vol. 68, No. 12, 8174–8179, Dec. 2020.
6. Fakhte, S., H. Oraizi, and R. Karimian, "A novel low-cost circularly polarized rotated stacked dielectric resonator antenna," *IEEE Antennas Wireless Propag. Lett.*, Vol. 13, 722–725, 2014.
7. Chowdhury, R. and R. K. Chaudhary, "An approach to generate circular polarization in a modified cylindrical-shaped dielectric resonator antenna using PMC boundary approximation," *IEEE Antennas Wireless Propag. Lett.*, Vol. 17, No. 9, 1727–1731, Sept. 2018.
8. Liu, Y., K. W. Leung, J. Ren, and Y. Sun, "Linearly and circularly polarized filtering dielectric resonator antennas," *IEEE Trans. Antennas Propag.*, Vol. 67, No. 6, 3629–3640, Jun. 2019.
9. Lin, C. and J. Sun, "Circularly polarized dielectric resonator antenna fed by off-centered microstrip line for 2.4-GHz ISM band applications," *IEEE Antennas Wireless Propag. Lett.*, Vol. 14, 947–949, Dec. 2015.
10. Lee, J. M., et al., "Circularly polarized semi-eccentric annular dielectric resonator antenna for X-band applications," *IEEE Antennas Wireless Propag. Lett.*, Vol. 14, 1810–1813, 2015.
11. Motevasselian, A., A. Ellgardt, and B. L. G. Jonsson, "A circularly polarized cylindrical dielectric resonator antenna using a helical exciter," *IEEE Trans. Antennas Propag.*, Vol. 61, No. 3, 1439–1443, Mar. 2013.
12. Altaf, A., Y. Yang, K. Lee, and K. C. Hwang, "Circularly polarized spidron fractal dielectric resonator antenna," *IEEE Antennas Wireless Propag. Lett.*, Vol. 14, 1806–1809, 2015.
13. Wang, K. X. and H. Wong, "A circularly polarized antenna by using rotated-stair dielectric resonator," *IEEE Antennas Wireless Propag. Lett.*, Vol. 14, 787–790, 2015.
14. Kumar, R. and R. K. Chaudhary, "A wideband circularly polarized cubic dielectric resonator antenna excited with modified microstrip feed," *IEEE Antennas Wireless Propag. Lett.*, Vol. 15, 1285–1288, 2016.
15. Zou, M., J. Pan, and Z. Nie, "A wideband circularly polarized rectangular dielectric resonator antenna excited by an archimedean spiral slot," *IEEE Antennas Wireless Propag. Lett.*, Vol. 14, 446–449, 2015.
16. Sharma, A., G. Das, S. Gupta, and R. K. Gangwar, "Quad-band quad-sense circularly polarized dielectric resonator antenna for GPS/CNSS/WLAN/WiMAX applications," *IEEE Antennas Wireless Propag. Lett.*, Vol. 19, No. 3, 403–407, Mar. 2020.
17. Varshney, G., V. S. Pandey, R. S. Yaduvanshi, and L. Kumar, "Wide band circularly polarized dielectric resonator antenna with stair-shaped slot excitation," *IEEE Trans. Antennas Propag.*, Vol. 65, No. 3, 1380–1383, Mar. 2017.
18. Lu, L., Y. Jiao, H. Zhang, R. Wang, and T. Li, "Wideband circularly polarized antenna with stair-shaped dielectric resonator and open-ended slot ground," *IEEE Antennas Wireless Propag. Lett.*, Vol. 15, 1755–1758, 2016.
19. Khalily, M., M. R. Kamarudin, and M. H. Jamaluddin, "A novel square dielectric resonator antenna with two unequal inclined slits for wideband circular polarization," *IEEE Antennas Wireless Propag. Lett.*, Vol. 12, 1256–1259, 2013.

20. Yang, M., Y. Pan, Y. Sun, and K. Leung, "Wideband circularly polarized substrate-integrated embedded dielectric resonator antenna for millimeter-wave applications," *IEEE Trans. Antennas Propag.*, Vol. 68, No. 2, 1145–1150, Feb. 2020.
21. Illahi, U., J. Iqbal, M. I. Sulaiman, M. M. Alam, M. M. Su'ud, and M. H. Jamaluddin, "Singly-fed rectangular dielectric resonator antenna with a wide circular polarization bandwidth and beamwidth for WiMAX/satellite applications," *IEEE Access*, Vol. 7, 66206–66214, 2019.
22. Trinh-Van, S., Y. Yang, K. Lee, and K. C. Hwang, "Single-fed circularly polarized dielectric resonator antenna with an enhanced axial ratio bandwidth and enhanced gain," *IEEE Access*, Vol. 8, 41045–41052, 2020.
23. Sun, W., W. Yang, P. Chu, and J. Chen, "Design of a wideband circularly polarized stacked dielectric resonator antenna," *IEEE Trans. Antennas Propag.*, Vol. 67, No. 1, 591–595, Jan. 2019.
24. Yang, M., Y. Pan, and W. Yang, "A singly fed wideband circularly polarized dielectric resonator antenna," *IEEE Antennas Wireless Propag. Lett.*, Vol. 17, No. 8, 1515–1518, Aug. 2018.
25. Lin, A., et al., "An L-shaped circularly polarized slot antenna," *Proc. IEEE Antennas Propag. Soc. Int. Symp.*, Vol. 4, 2786–2789, 1999.
26. Mu, C., S. Fang, H. Liu, Z. Wang, and S. Fu, "3-D-printed dielectric lens with cone-shaped cavity for axial ratio beamwidth enhancement of circularly polarized patch antenna," *IEEE Access*, Vol. 7, 105062–105071, 2019.